Inorg. Chem. **2003**, *42*, 7945–7950

A Stable Monomeric Nickel Borohydride

Patrick J. Desrochers,* Stacey LeLievre, Rosemary J. Johnson, Brian T. Lamb, Andrea L. Phelps, A. W. Cordes,† Weiwei Gu,‡ and Stephen P. Cramer‡

Department of Chemistry, University of Central Arkansas, Conway, Arkansas 72035

Received June 17, 2003

A stable discrete nickel borohydride complex (Tp*NiBH$_4$ or Tp*NiBD$_4$) was prepared using the nitrogen-donor ligand hydrotris(3,5-dimethylpyrazolyl)borate (Tp*$^-$). This complex represents one of the best characterized nickel(II) borohydrides to date. Tp*NiBH$_4$ and Tp*NiBD$_4$ are stable toward air, boiling water, and high temperatures (mp > 230 °C dec). X-ray crystallographic measurements for Tp*NiBH$_4$ showed a six-coordinate geometry for the complex, with the nickel(II) center facially coordinated by three bridging hydrogen atoms from borohydride and a tridentate Tp*$^-$ ligand. For Tp*NiBH$_4$, the empirical formula is $C_{15}H_{26}B_2N_6Ni$, $a = 13.469(9)$ Å, $b = 7.740(1)$ Å, $c = 18.851(2)$ Å, $\beta = 107.605(9)°$, the space group is monoclinic $P2_1/c$, and $Z = 4$. Infrared measurements confirmed the presence of bridging hydrogen atoms; both ν(B–H)$_{terminal}$ and ν(B–H)$_{bridging}$ are assignable and shifted relative to ν(B–D) of Tp*NiBD$_4$ by amounts in agreement with theory. Despite their hydrolytic stability, Tp*NiBH$_4$ and Tp*NiBD$_4$ readily reduce halocarbon substrates, leading to the complete series of Tp*NiX complexes (X = Cl, Br, I). These reactions showed a pronounced hydrogen/deuterium rate dependence ($k_H/k_D \approx 3$) and sharp isosbestic points in progressive electronic spectra. Nickel K-edge X-ray absorption spectroscopy (XAS) measurements of a hydride-rich nickel center were obtained for Tp*NiBH$_4$, Tp*NiBD$_4$, and Tp*NiCl. X-ray absorption near-edge spectroscopy results confirmed the similar six-coordinate geometries for Tp*NiBH$_4$ and Tp*NiBD$_4$. These contrasted with XAS results for the crystallographically characterized pseudotetrahedral Tp*NiCl complex. The stability of Tp*Ni-coordinated borohydride is significant given this ion's accelerated decomposition and hydrolysis in the presence of transition metals and simple metal salts.

Introduction

Nickel−hydrogen interactions have significant commercial, synthetic, and biochemical applications. Some include industrial hydrogenation,[1] nickel hydride rechargeable batteries,[2] hydrogen-storage media for fuel cells,[3] and bacterial nickel hydrogenase enzymes.[4] Borohydride ion can be the hydrogen source in some of these applications, and its reactivity with organic substrates is often enhanced in the presence of transition metals such as nickel.[5]

Lacking the protection of ancillary ligands, nickel(II) is reduced by borohydride ion to Raney nickel (a mixed metal/metal hydride) or nickel boride, Ni_2B; both exhibit significant catalytic hydrogenation activity. The recent application of Raney nickel to the reductive desulfurization of proteins is a promising tool in peptide syntheses.[6] Nickel boride chemistry has been reviewed,[5] and this material continues to receive attention for applications ranging from magnetic nanoparticles[7] to polymer-supported nickel boride catalysts for organic syntheses.[8]

Ancillary ligands help stabilize metal-coordinated borohydride, preventing both reduction to metals/metal hydrides and usually increasing the hydrolytic stability of the borohydride ion. Accordingly borohydride complexes of varying stability and reactivity are known for the majority of transition metals.[9] Three-centered two-electron bonding predominates in metal borohydrides, leading to a variety of

* Author to whom correspondence should be addressed. E-mail: patrickd@mail.uca.edu.

† Department of Chemistry, University of Arkansas, Fayetteville, AR 72701-1201.

‡ Department of Applied Sciences, University of California, Davis, CA 95616.

(1) *Catalysis of Organic Reactions*; Ford, M., Ed.; Marcel Dekker Inc.: New York, 2000; Vol. 82.
(2) Linden, D.; Reddy, T. *Handbook of Batteries*; McGraw-Hill: New York, 2002.
(3) Häussermann, U.; Blomqvist, H.; Noréus, D. *Inorg. Chem.* **2002**, *41*, 3684.
(4) Stadler, C.; de Lacey, A. L.; Montet, Y.; Volbeda, A.; Fontecilla-Camps, J. C.; Conesa, J. C.; Fernández, V. M. *Inorg. Chem.* **2002**, *41*, 4424
(5) Ganem, B.; Osby, J. O. *Chem. Rev.* **1986**, *86*, 763.
(6) Yan, L. Z.; Dawson, P. E. *J. Am. Chem. Soc.* **2001**, *123*, 526.
(7) Legrand, J.; Taleb, A.; Gota, S.; Guittet, M.-J.; Petit, C. *Langmuir* **2002**, *18*, 4131.
(8) Sim, T. B.; Choi, J.; Joung, M. J.; Yoon, N. M. *J. Org. Chem.* **1997**, *62*, 2357.

10.1021/ic034687a CCC: $25.00
Published on Web 10/29/2003

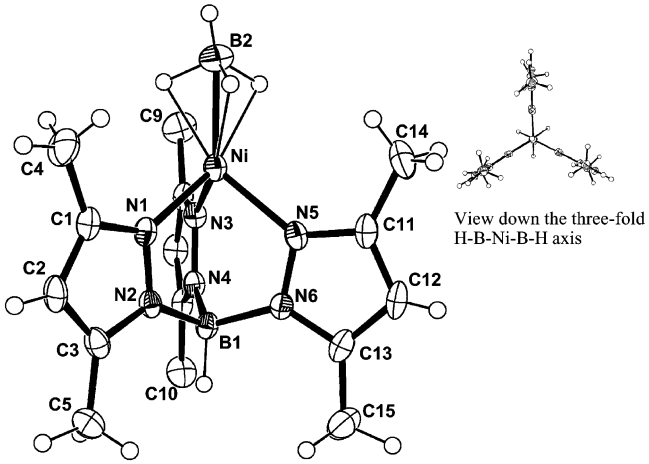

Figure 1. ORTEP sketches of Tp^*NiBH_4 (50% probability ellipsoids). Hydrogen atoms and some carbon labels on the back pyrazole ring are omitted for clarity.

hapticities. $(COT)Nd(\eta^3\text{-}BH_4)(THF)_2$ is a more recent example[10] from the extensive list of f-block borohydride complexes.[11] $Tp^*Cd(\eta^2\text{-}BH_4)$ is susceptible to further reduction, yielding cadmium−cadmium-bonded products.[12] A particularly active borohydride complex of titanium is $(^iPrO)_2Ti(\eta^2\text{-}BH_4)$; this complex reduces some organic carbonyls more efficiently than strong hydride sources such as $LiAlH_4$.[13] Borohydride hapticity in the d^8 $(Ph_3P)_3Co(\eta^1\text{-}BH_4)$ was inferred on the basis of electronic spectroscopy comparisons to $(Ph_3P)_3CoX$ (X = Cl, Br, I).[14] Not surprisingly low-valent metal(I) borohydrides are stabilized by phosphorus and arsenic donors,[14,15] whereas nitrogen donors tend to resist metal reduction[16] and stabilize higher valent metal borohydrides as in the present work.

A stable monomeric nickel borohydride, Tp^*NiBH_4 (Figure 1),[17] is described, representing the best characterized nickel borohydride complex to date. The protection afforded by the facial-N_3 donor is significant given the demonstrated propensity of the nickel(II) ion for extensive reduction by borohydride. The stable hydrogen-rich nickel environment of Tp^*NiBH_4 was probed by both single-crystal X-ray diffraction and nickel K-edge X-ray absorption spectroscopy (XAS) measurements, a technique frequently applied as a site-specific probe in nickel−iron hydrogenase enzymes.[18] Tp^*NiBH_4 also cleanly reduces halocarbons, a characteristic of metal hydrides,[19] Raney nickel, nickel boride,[5] and square-planar nickel cyclam complexes.[20]

Experimental Section

Materials and Methods. Reagents and solvents were obtained from Aldrich Chemical Co. and Fisher Scientific and used as received. The potassium salt of hydrotris(3,5-dimethylpyrazolyl)-borate (KTp*) was prepared according to literature methods via the molten reaction of excess pyrazole and potassium borohydride.[21] This KTp* salt was used to prepare Tp^*NiNO_3 according to the method of Parkin et al.[22] Inert atmosphere work employed standard Schlenk techniques, glassware, and an inert gas/vacuum manifold.

UV−Vis, IR, and NMR Spectroscopy. Electronic spectra were recorded on a Varian Cary 50 spectrometer using 1 cm quartz cells. Infrared spectra were recorded using a Nicolet Magna 560 FT spectrometer with samples either as KBr pellets or as dichloromethane solutions using a solution cell fitted with NaCl windows. NMR spectra were recorded in deuteriochloroform on a JEOL ECX 300 MHz FT-NMR spectrometer. All spectroscopic measurements were recorded at ambient temperatures.

Synthesis of Tp^*NiBH_4. Tp^*NiBH_4 was synthesized using equimolar amounts of Tp^*NiNO_3 (600 mg, 1.4 mmol) and $NaBH_4$ (54 mg, 1.4 mmol). Each was dissolved in a minimal amount of acetonitrile, and the sodium borohydride solution was added dropwise to the teal-blue-colored Tp^*NiNO_3 solution. A dark green reaction mixture was formed, and a bright green solid product precipitated. After the reaction mixture was cooled on ice for 10 min, the solid was separated by centrifugation. The product was washed twice with water and twice with ice cold acetonitrile and then dried with a nitrogen stream. This material was redissolved in dichloromethane, and the resulting solution was dried further using anhydrous calcium sulfate. Evaporation of this dry solution yielded the product as a bright green solid, 300 mg (60%). Anal. Expt (Theory): C, 49.1 (48.6); H, 7.4 (7.1); N, 23.0 (22.7). Mp: >230 °C dec. IR: (Tp^{*-}) $\nu(B-H) = 2530\ cm^{-1}$ (in CH_2Cl_2) and 2515 cm^{-1} (KBr pellet).

Tp^*NiBD_4 was prepared via the same procedure using sodium borodeuteride (Aldrich).

Synthesis and Purification of Tp*NiCl. This compound was prepared by reacting Tp^*NiBH_4 with neat chloroform or carbon tetrachloride. A typical reaction involved the dissolution of Tp^*NiBH_4 in the chlorocarbon solvent; the initially bright green solution changed to bright pink in a matter of minutes, and when the solution was sufficiently concentrated, clear effervescence was observed. The reaction in carbon tetrachloride was complete in less than 2 min at ambient temperature (ca. 23 °C). In chloroform elevated temperatures were required (50 °C). Evaporation of the reaction solvent yielded the crude product as a pink solid. This solid was purified by column chromatography (80:20 chloroform/methanol mobile phase, 3 cm × 20 cm column made from 70−270 mesh 60 Å silica gel as the stationary phase). While in contact with Lewis basic solvents and while eluting down the column, pink

(9) Marks, T. J.; Kolb, J. R. *Chem. Rev.* **1977**, *77*, 263.
(10) Cendrowski-Guillaume, S. M.; Nierlich, M.; Lance, M.; Ephritikhine, M. *Organometallics* **1998,** *17*, 786. COT = cyclooctatetraene dianion.
(11) Banks, R. H.; Edelstein, N. M.; Spencer, B.; Templeton, D. H.; Zalkin, A. *J. Am. Chem. Soc.* **1980**, *102*, 620.
(12) Reger, D. L.; Mason, S. S.; Rheingold, A. L. *J. Am. Chem. Soc.* **1993**, *115*, 10406.
(13) Ravikumar, K. S.; Chandrasekaran, S. *J. Org. Chem.* **1996,** *61*, 826.
(14) Holah, D. G.; Hughes, A. N.; Hui, B. C.; Wright, K. *Can. J. Chem.* **1974**, *52*, 2990.
(15) Dapporto, P.; Midollini, S.; Orlandini, A.; Sacconi, L. *Inorg. Chem.* **1976**, *15*, 2768.
(16) Curtis, N. F. *J. Chem. Soc.* **1965**, 924.
(17) Ligand abbreviations are after Trofimenko, S. *Scorpionates: The Coordination Chemistry of Polypyrazolborate Ligands*; Imperial College Press: River Edge, NJ, 1999. Tp^{*-} = hydrotris(3,5-dimethylpyrazolyl)borate.
(18) (a) Gu, W.; Jacquamet, L.; Patil, D. S.; Wang, H. -X.; Evans, D. J.; Smith, M. C.; Millar, M.; Koch, S.; Eichhorn, D. M.; Latimer, M.; Cramer, S. P. *J. Inorg. Biochem.* **2003**, *93*, 41. (b) Davidson, G.; Choudhury, S. B.; Gu, Z.; Bose, K.; Roseboom, W.; Albracht, S. P. J.; Maroney, M. J. *Biochemistry* **2000**, *39*, 7468. (c) Amara, P.; Volbeda, A.; Fontecilla-Camps, J. C.; Field, M. J. *J. Am. Chem. Soc.* **1999**, *121*, 4468. (d) Gu, Z.; Dong, J.; Allan, C. B.; Choudhury, S. B.; Franco, R.; Moura, J. J. G.; Moura, I.; LeGall, J.; Przybyla, A. E.; Roseboom, W.; Albracht, S. P. J.; Axley, M. J.; Scott, R. A.; Maroney, M. J. *J. Am. Chem. Soc.* **1996**, *118*, 11155.
(19) Cha, M.; Gatlin, C. L.; Critchlow, S. C.; Kovacs, J. A. *Inorg. Chem.* **1993**, *32*, 5868.
(20) Stolzenberg, A. M.; Zhang, Z. *Inorg. Chem.* **1997**, *36*, 593.
(21) Trofimenko, S. *J. Am. Chem. Soc.* **1967**, *89*, 6288.
(22) Han, R.; Looney, A.; McNeil, K.; Parkin, G.; Rheingold, A. L.; Haggerty, B. S. *J. Inorg. Biochem.* **1993**, *49*, 105.

Table 1. Crystal, Collection, and Refinement Parameters for Tp*$NiBH_4$ and Tp*NiCl

	Tp*$NiBH_4$	Tp*NiCl
empirical formula	$C_{15}H_{26}B_2N_6Ni$	$C_{15}H_{22}BClN_6Ni$
fw	370.75	391.36
cryst size, mm	0.1 × 0.1 × 0.1	0.34 × 0.20 × 0.16
a, Å	13.469(9)	17.4467(4)
b, Å	7.7400(11)	13.1553(2)
c, Å	18.851(2)	8.0191(7)
β, deg	107.605(9)	90
V, Å^3	1873.2(13)	1840.52(17)
2θ for cell, deg	4−52	4−52
d(calcd), g/cm^3	1.315	1.412
cell measmt temp, K	173	293
space group	monoclinic, $P2_1/c$	orthorhombic, $P2_1ma$
Z	4	4
λ(Mo Kα), Å	0.7107	0.7107
h, *k*, *l* min to max ranges	$h = -16$ to $+16$ $k = -9$ to $+9$ $l = -23$ to $+22$	$h = -23$ to $+23$ $k = -17$ to $+17$ $l = -10$ to $+10$
max 2θ, deg	52	60
no. of unique reflns	3673	2547
no. of reflns refined [$I > 2.0\sigma$(I)]	2947	2093
R, R_w[a] (for all reflns)	0.088, 0.104	0.048, 0.094
R, R_w[a] (for $I > 2.0\sigma(I)$]	0.056, 0.092	0.036, 0.089
no. of params refined	321	261
GOF	1.161	1.079
final diff map, e/Å^3	−0.36, 0.50	−0.53, 0.60

[a] $R = \sum[(|F_o| - |F_c|)]/\sum|F_o|$. $R_w = \{[\sum[w(F_o^2 - F_c^2)^2]/\sum[w(F_o^2)^2]\}^{1/2}$. $w = 1/[\sigma^2F_o^2 + (nP)^2]$. $P = (F_o^2 + 2F_c^2)/3$. $n = 0.0433$ for Tp*$NiBH_4$ and $n = 0.0445$ for Tp*NiCl.

Tp*NiCl appears blue and exhibits electronic spectra typical of six-coordinate nickel(II) centers. Evaporation of this solvent returns the original pink Tp*NiCl product. Anal. Expt (Theory): C, 45.6 (46.0); H, 5.7 (5.7); N, 21.2 (21.5).

Tp*NiBr and Tp*NiI were prepared via a similar procedure at ambient temperature using neat bromoform, carbon tetrabromide dissolved in dichloromethane, neat iodomethane, or iodoform dissolved in dichloromethane. These too are purified readily by column chromatography.

X-ray Crystallography. A green block crystal of Tp*$NiBH_4$ measuring 0.10 mm × 0.10 mm × 0.10 mm was grown from slow evaporation of a dichloromethane solution of the compound. A total of 3673 unique reflections (2947 with $I > 2\sigma$) were collected at 173(2) K using a Rigaku mercury CCD diffractometer. The structure was solved by direct methods using SHELX software. All non-hydrogen atoms were refined anisotropically. Hydrogen atoms of the coordinated BH_4^- were located on a final difference map; these atoms represent four of the top five electron density peaks on the difference map. All hydrogen atoms were refined isotropically. Results are summarized in Tables 1 and 2.

A rose-colored crystal of Tp*NiCl measuring 0.34 mm × 0.20 mm × 0.16 mm was grown from slow evaporation of a dichloromethane solution of the compound. A total of 2547 unique reflections (2093 with $I > 2\sigma$) were collected at ambient temperature using a Rigaku mercury CCD diffractometer. The structure was solved by direct methods using SHELX software, and all non-hydrogen atoms were refined anisotropically. Results are summarized in Tables 1 and 2.

Kinetic Measurements. The reaction of Tp*$NiBH_4$ with halocarbons is fast in neat halocarbon solvents that are open to the air and essentially instantaneous under inert atmospheres. The stable free radical TEMPO (2,2,6,6-tetramethyl-1-piperidinyloxyl) was used to slow the reaction under a nitrogen atmosphere to more manageable times of 5−10 min. A typical run used a reaction mixture that was 1 mM in Tp*$NiBH_4$, 1 mM in TEMPO, and 50−60 mM in CX_4 (X = Cl, Br), all prepared under nitrogen in degassed dichloromethane. Absorbance readings at 500 nm were made on this mixture loaded into a septum-fitted quartz cuvette. All of the A_{500} vs time plots had sigmoidal profiles, with the reaction reaching a maximal rate at an approximately 30% extent of reaction.

X-ray Absorption Spectroscopy. The Ni K-edge spectra were recorded at beamline 7-3 at the Stanford Synchrotron Radiation Laboratory (SSRL). Si(220) monochromator crystals were used with 2 mm slits. The energy was calibrated using Ni foil as an internal standard in a three-ion-chamber geometry, and the energy scale was calibrated using 8331.6 eV as the first inflection point of the Ni foil spectrum. All ion chambers were filled with N_2. Harmonic rejection was accomplished by detuning the second monochromator crystal to 50% of the maximum possible flux. Spectra were recorded from 8250 to 9400 eV in 30 min scans (3−4 scans per sample). The extended X-ray absorption fine structure (EXAFS) oscillations were extracted from the averaged spectra using the EXAFSPAK analysis software (courtesy of G. N. George), using 8350 eV as an initial E_0 for defining the photoelectron wave vector. The resultant EXAFS data were weighted by k^3 and Fourier transformed over the region $k = 1-16.5$ Å^{-1}. Least-squares fits of the EXAFS data were performed. The phase shift and amplitude were calculated using the program FEFF v. 7.

Results and Discussion

The six-coordinate nickel center in Tp*$NiBH_4$ is bound by three nitrogen atoms of Tp*$^-$ and three bridging hydrides of BH_4^-. The compound is synthesized by simple ligand metathesis from Tp*$NiNO_3$ or Tp*NiX (X = Cl or Br). Tp*$NiBH_4$ is stable toward heat (mp > 230 °C dec), moisture, and air. This stability is unusual compared to the lower hydrolytic stability of Tm*$LiBH_4$[23] and the nickel(I) borohydride $(Ph_3P)_3NiBH_4$.[14] The higher charge of the nickel(II) might be expected to encourage hydride liberation from the coordinated BH_4 ligand, and yet this compound is stable indefinitely. The reaction of nickel(II) absent the protection afforded by Tp*$^-$ readily yields reduced nickel solids via a route known for the production of Raney nickel and nickel boride.[6] This stability likely explains the inability (to date) of Tp*$NiBH_4$ to catalyze hydrogenation reactions, which is a reported characteristic of nickel borides and Raney nickel.

Table 2. Selected Bond Distances (Å) and Angles (deg) in Tp*$NiBH_4$ and Tp*NiCl[a]

Tp*$NiBH_4$				Tp*NiCl			
Ni−N1	1.997(3)	B2−Ni−N1	123.1(2)	Ni−N1	1.964(3)	Cl−Ni−N1	123.7(2)
Ni−N3	1.996(3)	B2−Ni−N3	123.3(2)	Ni−N3	1.962(3)	Cl−Ni−N3	122.4(2)
Ni−N5	2.009(3)	B2−Ni−N5	127.6(2)				
Ni−B2	2.048(5)			Ni−Cl	2.17(2)		
Ni−H	1.87(4)−1.94(7)						

[a] Estimated standard deviations in parentheses.

Infrared measurements indicated $\nu(B-H)_{terminal}$ as a shoulder at 2500 cm^{-1} near the strong $\nu(B-H)$ of the Tp^{*-} ligand at 2515 cm^{-1}. The $\nu(B-D)_{terminal}$ of Tp^*NiBD_4 is shifted to 1890 cm^{-1} in good agreement with published $\nu(B-H,D)$ shifts and theory.[24] A doublet at 2110 and 2063 cm^{-1} is indicative of tridentate $\nu(B-H)_{bridging}$.[9] The $\nu(B-D)_{bridging}$ band of Tp^*NiBD_4 is expected to shift to a region obscured by strong Tp^{*-} vibrations.[24] Upon reaction of Tp^*NiBH_4 with halocarbons, these $\nu(B-H,D)$ bands disappear.

X-ray crystallography confirmed the six-coordinate nickel geometry of Tp^*NiBH_4 (Figure 1). Both ligands coordinate nickel as facial donors, resulting in nearly perfect C_{3v} symmetry with a H−B−Ni−B−H principal axis. Nickel−nitrogen distances (average of 2.001(3) Å) for Tp^*NiBH_4 are typical of nickel in pseudotetrahedral geometries.[25] Hydrogen atoms for the η^3-BH_4 ligand were located on a difference map and refined well. The nickel−hydrogen distances in Tp^*NiBH_4 range from 1.87(4) to 1.94(7) Å and are comparable to other nickel−hydrogen distances (1.863(9) Å) in nickel hydroborates.[26]

Tp^*NiBH_4 is a structural analogue of $Tm^*Li(\eta^3\text{-}BH_4)$.[23] Both complexes contain metal ions in trigonal $N_3(\eta^3\text{-}BH_4)$ coordination spheres. Despite comparable molecular volumes (482 $Å^3$ for $Tm^*Li(\eta^3\text{-}BH_4)$ and 468 $Å^3$ for Tp^*NiBH_4) and comparable average metal−nitrogen distances (2.056(6) Å for Li−N and 2.001(3) for Ni−N), the metal−boron and metal−hydride distances are significantly longer in the lithium complex (Li−H = 2.1 Å and Li−B = 2.223(7) Å), much longer than is explained by the slight difference in these metals' ionic radii.[27] The shorter Ni−BH_4 contact (Ni−B = 2.048(5) Å) could result from the greater electrostatic pull from the divalent nickel center; however, the Ni−B distance is within the covalent range expected from the larger boron (vs nitrogen) covalent radius.[28] The covalent interaction implied by the short metal−boron contacts in Tp^*NiBH_4 may be a factor in the reactivity observed for this complex and one reason for the contrasting lower stability of the more ionic lithium form.[23]

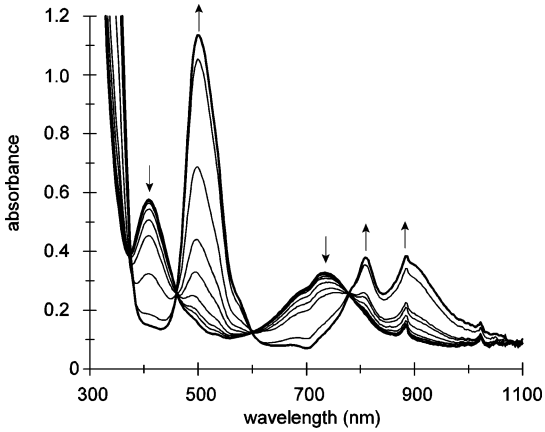

Figure 2. Successive electronic spectra of the $Tp^*NiBH_4 + CBr_4$ reaction mixture in dichloromethane (TEMPO added, under nitrogen). Initial: Tp^*NiBH_4, λ_{max} at 410 nm (ϵ = 160 M^{-1} cm^{-1}) and 732 (86). Final: Tp^*NiBr, λ_{max} at 500 nm (230), 810 (70), and 894 (65). Isosbestic points are seen at 374, 460, 600, and 780 nm.

The electronic spectrum of Tp^*NiBH_4 is not easily described by either a four-coordinate T_d or a six-coordinate O_h model (Figure 2). Extinction coefficients for the two visible transitions are in the range expected for pseudo-T_d nickel(II) complexes.[29] However, unreasonable Δ_T and B values are derived when the bands are fitted to the two highest energy d^8 T_d transitions: $^3A_2 \leftarrow {}^3T_1(F)$ (732 nm) and $^3T_1(P) \leftarrow {}^3T_1(F)$ (410 nm). Assigning these transitions to the two highest energy d^8 O_h transitions, $^3T_1(F) \leftarrow {}^3A_2$ (410 nm) and $^3T_1(P) \leftarrow {}^3A_2$ (732 nm), yields reasonable Δ_O = 7760 cm^{-1} and B = 935 cm^{-1} values. The preference by nickel(II) for nitrogen over $-BH_3$ coordination was demonstrated by $Ni(en)_2Cl_2$. This complex binds the ambidentate ligand $NCBH_3$ exclusively through the nitrogen donors, as evidenced by the purple color of $(en)_2Ni(NCBH_3)_2$;[30] purple and lavender colors are classic characteristics of octahedral NiN_6 geometries such as $Ni(en)_3^{+2}$, $Ni(NH_3)_6^{+2}$, and $(Tp^*)_2Ni$. Nitrogen donor ligands yield some of the largest values of Δ_O for nickel(II) ($\Delta_O \approx 10-12000$ cm^{-1}).[29] Therefore, the lower value of Δ_O observed for Tp^*NiBH_4 is consistent with the weak ligand field observed for the H_3B-X tripod toward nickel(II).

The ability to convert $CHCl_3$ to CH_2Cl_2 is a reported characteristic of transition-metal hydrides.[19] Room temperature titrations under an inert nitrogen atmosphere in dichloromethane (10−15 mM reagent concentrations) yielded the following reaction stoichiometries (±10%): CCl_4:Tp^*NiBH_4 = 1:1, CBr_4:Tp^*NiBH_4 = 1:2, and $HCBr_3$:Tp^*NiBH_4 = 1:1. Tp^*NiBH_4 reacts with chloroform but only at elevated temperatures (>50 °C), and dichloromethane is unreactive even at reflux for several hours. ^1H NMR

(23) Reger, D. L.; Collins, J. E.; Matthews, M. A.; Rheingold, A. L.; Liable-Sands, L. M.; Guzei, I. A. *Inorg. Chem.* **1997**, *36*, 6266. Tm* is hydrotris(3,5-dimethylpyrazolyl)methane, the neutral carbon analogue of Tp^{*-}.

(24) The symmetric $\nu(B-H,D)$ stretch for $^{10}BH_4^-$ is 2270 cm^{-1}, and that for $^{10}BD_4^-$ is 1604 cm^{-1}, giving a ν_{B-D}/ν_{B-H} ratio of 0.71: Nakamoto, K. *Infrared and Raman Spectra of Inorganic and Coordination Compounds*, 4th ed.; Wiley-Interscience: New York, 1986; p 131. ν_{B-D}/ν_{B-H} = 0.753(2): Segal, B. G.; Lippard, S. J. *Inorg. Chem.* **1977**, *16*, 1623. Hook's law predicts a ν_{B-D}/ν_{B-H} ratio of 0.74. Using this as a rough guide, $\nu(B-D)_{bridging}$ for Tp^*NiBD_4 is estimated to lie near 1530 cm^{-1} (0.74$\nu(B-H)_{bridging}$ at 2063 cm^{-1} is 1530 cm^{-1}).

(25) Four-coordinate (pseudo-T_d) nickel−nitrogen distances are typically ≤2 Å, whereas five- and six-coordinate nickel−nitrogen distances range from 2.02 to 2.17 Å: (a) Desrochers, P. J.; Cutts, R. W.; Rice, P. K.; Golden, M. L.; Graham, J. B.; Barclay, T. M.; Cordes; A. W. *Inorg. Chem.* **1999**, *38*, 5690−5694. (b) Trofimenko, S.; Calabrese, J. C.; Kochi, J. K.; Wolowiec, S.; Hulsbergen, F. B.; Reedijk, J. *Inorg. Chem.* **1992**, *31*, 3943. (c) Hikichi, S.; Yoshizawa, M.; Sasakura, Y.; Akita, M.; Moro-oka, Y. *J. Am. Chem. Soc.* **1998**, *120*, 10567. (d) Bandoli, G.; Clemente, D. A.; Paolucci, G.; Doretti, L. *Cryst. Struct. Commun.* **1979**, *8*, 965. (e) Calabrese, J. C.; Trofimenko, S. *Inorg. Chem.* **1992**, *31*, 4810. (f) Calabrese, J. C.; Domaille, P. J.; Thompson, J. S.; Trofimenko, S. *Inorg. Chem.* **1990**, *29*, 4429. See also ref 22.

(26) Alvarez, H. M.; Krawiec, M.; Donovan-Merkert, B. T.; Fouzi, M.; Rabinovich, D. *Inorg. Chem.* **2001**, *40*, 5736.

(27) Shannon, R. D. *Acta Crystallogr.* **1976**, *A32*, 751. Six-coordinate ionic radii are (Li^+) 0.90 Å and (Ni^{2+}) 0.83 Å.

(28) Covalent single bond radii: boron, 0.88 Å; nitrogen, 0.70 Å. Muetterties, E. L. *The Chemisty of Boron and its Compounds*; John Wiley & Sons: New York, 1967; p 377.

(29) Lever, A. B. P. *Inorganic Electronic Spectroscopy*; Elsevier: New York, 1968. Spin-allowed d to d extinction coefficients range from 100 to 200 M^{-1} cm^{-1} for T_d nickel(II) (p 342) and from 5 to 30 M^{-1} cm^{-1} for O_h nickel(II) (p 334). The free nickel(II) ion B = 1041 cm^{-1} (p 164).

(30) Lippard, S. J.; Welcker, P. S. *Chem. Commun.* **1970**, 515.

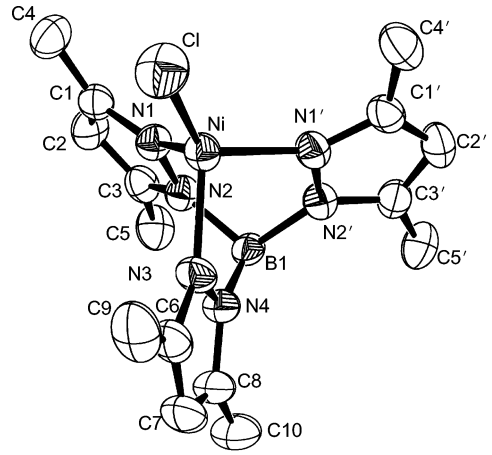

Figure 3. ORTEP sketch of Tp*NiCl (50% probability ellipsoids). Hydrogen atoms are omitted for clarity.

confirmed the formation of CH_2Cl_2 and very little $CHCl_3$ from CCl_4. When the reaction is rapid, as for CX_4 halocarbons, clear effervescence is observed, and the exothermicity of the reaction can be felt. The gas evolved from this reaction is IR-silent, and dissolved gas in the reaction mixture gave a singlet at 4.65 ppm in the ^{1}H NMR spectrum of the reaction mixture. Independent samples of 7 mM Tp*NiCl in chloroform sparged with H_2 gas reproduced this 4.65 ppm singlet. These observations are consistent with the formation of dihydrogen from these reactions.[31]

Halocarbon reductions by Tp*NiBH$_4$ involve at least one radical intermediate. Under an inert nitrogen atmosphere the reduction of CBr_4 is instantaneous; in air at the same concentrations, the reaction takes several minutes. TEMPO addition under nitrogen slows the reaction time from a few seconds to more than 10 min. A significantly slower reaction rate is observed when Tp*NiBH$_4$ is replaced with Tp*NiBD$_4$ (estimated $k_H/k_D = 3$), so that hydrogen atom or hydride ion transfer is integral to the rate-limiting step. The radical trap 2-methyl-2-nitrosopropane (MNP) was used in an attempt to observe the radical intermediate by electron paramagnetic resonance (EPR). In the presence of MNP and no TEMPO the reaction was again nearly instantaneous under nitrogen, and no distinct MNP radical signature could be observed by continuous-wave X-band EPR (Resonance Instruments model 8400) in these reaction mixtures at ambient temperature.

Electronic spectra of the TEMPO-slowed transformation from Tp*NiBH$_4$ to Tp*NiBr are summarized in Figure 2. The final spectrum is typical of C_{3v} Tp^{Y}Ni−X centers,[32] and the shift in transition wavelength for the Tp*Ni−X series (X = Cl, Br, I) matches the halide ligand field trend.[33] These spectra show a smooth transition from Tp*NiBH$_4$ to Tp*NiBr with several sharp isosbestic points. This implies no pronounced buildup of nickel-containing intermediates in the reaction mixture. However, a common feature of the TEMPO-slowed reaction is an induction period preceding a maximal rate that is reached at an about 30% extent of reaction. The changes in concentration of reactants and products with time have sigmoidal profiles reminiscent of autocatalytic processes.[34]

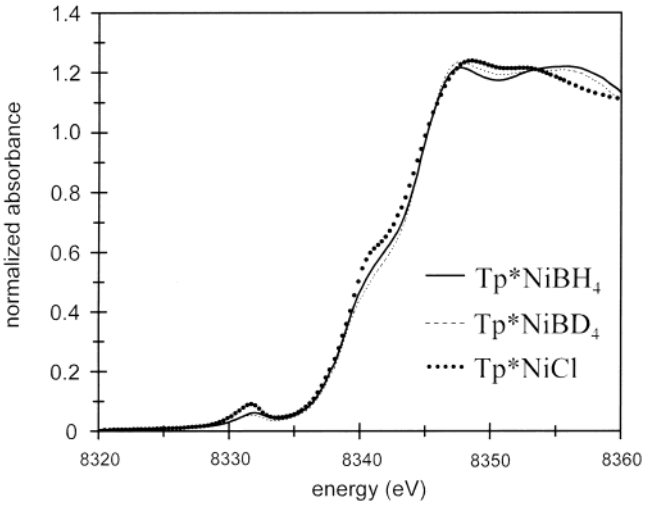

Figure 4. XAS spectra for Tp*Ni complexes.

Table 3. 1s to 3d Preedge X-ray Absorption Results

compound	1s to 3d peak energy (eV)	integrated[a] 1s to 3d intensity (eV)
Tp*NiBH$_4$	8332.0	0.086
Tp*NiBD$_4$	8331.9	0.057
Tp*NiCl	8331.7	0.162

[a] Using an arc tangent function from the absorption edge as a background, this peak was integrated from 8328 to 8335 eV.

A sample of Tp*NiCl isolated from a reaction mixture was analyzed by X-ray crystallography (Figure 3). The complex contains a nickel center bound by three nitrogen atoms of Tp*$^-$ and the single chlorine atom in a pseudotetrahedral array. Its nickel−chlorine length of 2.17(2) Å and short nickel−nitrogen distances compare favorably to those of pseudotetrahedral nickel(II).[25]

XAS spectra were recorded for Tp*NiBH$_4$, Tp*NiBD$_4$, and Tp*NiCl (Figure 4). All three displayed typical nickel(II) K-edge energies (8339−8340 eV)[35] and clear 1s → 3d preedge electronic transitions near 8332 eV. The more intense 1s → 3d transition for Tp*NiCl is consistent with its pseudotetrahedral geometry compared to the six-coordinate geometry of the borohydride and borodeuteride complexes (integrated intensities summarized in Table 3).[35] The EXAFS

(31) (a) Georgakaki, I. P.; Miller, M. L.; Darensbourg, M. Y. *Inorg. Chem.* **2003**, *42*, 2489. (b) Zhao, X.; Georgakaki, I.. P.; Miller, M. L.; Mejia-Rodriguez, R.; Chiang, C.-Y.; Darensbourg, M. Y. *Inorg. Chem.* **2002**, *41*, 3917.

(32) (a) Hammes, B. S.; Carrano, C. J. *Inorg. Chem.* **1999**, *38*, 3562. (b) Gerloch, M.; Hanton, L. R.; Manning, M. R. *Inorg. Chim. Acta* **1981**, *48*, 205. (c) Trofimenko, S.; Calabrese, J. C.; Thompson, J. S. *Inorg. Chem.* **1987**, *26*, 1507.

(33) In dichloromethane for Tp*NiCl λ_{max} = 485, 800, and 880 nm, for Tp*NiBr λ_{max} = 500, 810, and 894 nm, and for Tp*NiI λ_{max} = 530, 830, and 910 nm.

(34) (a) Acosta, A.; Zink, J. I.; Cheon, J. *Inorg. Chem.* **2000**, *39*, 427. (b) Steinfeld, J. I.; Francisco, J. S.; Hase, W. L. *Chemical Kinetics and Dynamics*, 2nd ed.; Prentice Hall: Upper Saddle River, NJ, 1999; p 151.

(35) Ni^0 K-edge absorption is at 8331 eV: (a) Colpas, G. J.; Maroney, M. J.; Bagyinka, C.; Kumar, M.; Willis, W. S.; Suib, S. L.; Baidya, N.; Mascharak, P. K. *Inorg. Chem.* **1991**, *30*, 920. (b) Gu, Z.; Dong, J.; Allan, C. B.; Choudhury, S. B.; Franco, R.; Moura, J. J. G.; Moura, I.; LeGall, J.; Przybyla, A. E.; Roseboom, W.; Albracht, S. P. J.; Axley, M. J.; Scott, R. A.; Maroney, M. J. *J. Am. Chem. Soc.* **1996**, *118*, 11155.

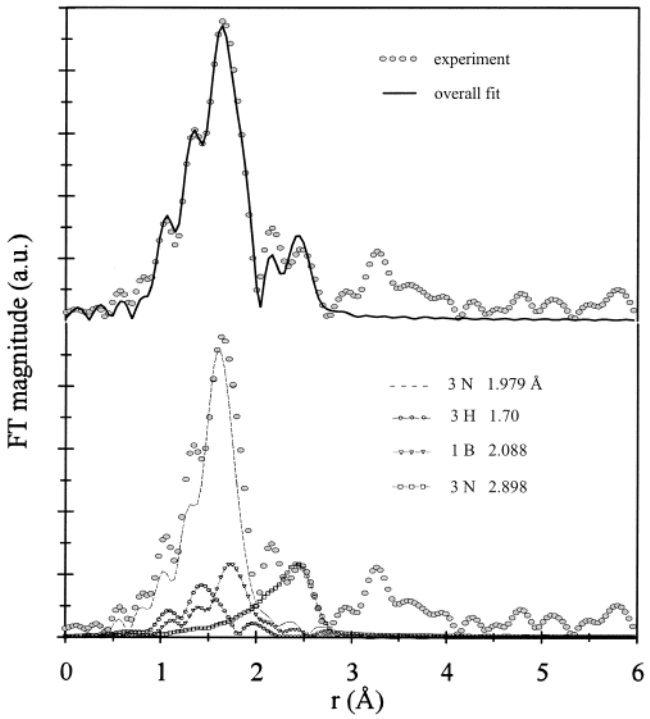

Figure 5. Fourier-transformed EXAFS spectra for Tp*NiBH$_4$. The top trace shows a comparison of experimental data and the full model fit. The bottom trace shows individual atom shell contributions and comparison to experimental data.

Table 4. Fourier-Filtered Ni EXAFS Data for Tp*Ni Complexes[a]

compound	N	r (Å)	$10^3\Delta\sigma^2$ (Å^2)	F	av crystallographic bond length (Å)
Tp*NiBH$_4$	3 N	1.998	1.67	209.5	2.001(3)
	3 N	2.925	5.36		2.890(4)
	3 N	1.989	1.45	179.8	2.001(3)
	3 N	2.907	4.78		2.890(4)
	3 H	1.709	0.18		1.909(4)
	3 N	1.979	1.24	158.8	2.001(3)
	3 N	2.898	4.94		2.890(4)
	3 H	1.695	0.7		1.909(4)
	1 B	2.088	1.0		2.048(5)
Tp*NiBD$_4$	3 N	2.004	1.83	221.5	
	3 N	2.937	6.10		
	3 N	2.001	1.49	202.0	
	3 N	2.925	5.18		
	3 H	1.744	1.68		
	3 N	1.985	1.94	175.1	
	3 N	2.905	4.82		
	3 H	1.707	1.0		
	1 B	2.088	1.0		
Tp*NiCl	3 N	1.960	5.16	265.4	1.963(3)
	1 Cl	2.147	3.65		2.17(2)
	3 N	2.844	4.38		2.833(4)
	1 B	3.055	−0.04		2.971(4)

[a] k range from 1 to 16.5 Å^{-1}. $F = \Sigma(\chi_{calcd} - \chi_{obsd})^2k^6$. σ^2 is the mean square deviation of r. χ is defined in ref 18a.

regions for Tp*NiCl and Tp*NiB(H,D)$_4$ reflect the significant differences in their nickel coordination spheres. FT EXAFS results for Tp*NiBH$_4$ are summarized in Figure 5, and iterative fit parameters for all three complexes are summarized in Table 4. Satisfactory Ni−N, Ni−B, and Ni−Cl bond lengths are obtained from these fits, independently confirming a covalent nickel−boron distance in the Tp*NiB(H,D)$_4$ complexes. Ni−H results from these data vary from the crystallographic values by at least 0.2 Å. Including the crystallographic results, a Ni−H distance of 1.8 ± 0.1 Å for Tp*NiBH$_4$ emerges and is within the range of 1.71−2.15 Å reported for 10 different Ni−H−B complexes.[36]

The hydrolytic stability of the borohydride ion in the presence of Lewis acids appears to depend on the degree of covalence of its interaction with M^{n+}. At the ionic extreme, unprotected alkali-metal borohydrides are easily hydrolyzed, and nickel(II) salts degrade borohydride en route to intractable but catalytically useful nickel borides and nickel/nickel hydrides.[7,8] Increased covalence of the Tm*M$^+$ moiety yields alkali-metal borohydride adducts with greater hydrolytic stability.[23] The present work suggests that increased covalence in Tp*NiBH$_4$ lessens the hydridic character of coordinated hydrogen atoms, perhaps instead encouraging atomic hydrogen (radical) reactivity.

Detailed descriptions of the bonding in Tp*NiBH$_4$ are warranted. Borohydride is an important reagent for this metal with rich hydrogen chemistry. It is also interesting to extrapolate results from coordinated borohydride to the isoelectronic methane molecule. Gas-phase measurements on CpCo$^+$ confirmed the formation of the simple methane adduct CpCoCH$_4^+$.[37] Unligated iron methane gas-phase adducts have also been observed.[38] Methane activation and H$_2$ elimination were observed for both systems, implying significant covalent interaction in these MCH$_4$ systems. Although no precise geometry was postulated for CpCoCH$_4^+$, η^3-CH$_4$ represents one possibility in light of the present results for Tp*NiBH$_4$ and the common facial coordination and six-electron donation of the Cp$^-$ and Tp*$^-$ ligands. Detailed magnetic resonance (^{1}H, ^{2}H, and ^{11}B NMR and high-frequency EPR) measurements on Tp*NiBH$_4$ and Tp*NiBD$_4$ are ongoing to better describe the electronic structure of the metal XH$_4$ manifold in this system.

Acknowledgment. Financial support was provided by the donors of the Petroleum Research Fund, administered by the American Chemical Society (Grant 35602-B3), the Arkansas Science Information Liaison Office, and the University of Central Arkansas Research Council (P.J.D.). Funding from the Arkansas Science and Technology Authority was used to purchase the X-ray diffractometer used in this work (A.W.C.). The FT NMR spectrometer used in this work was funded in part by the National Science Foundation (CCLI Grant 0125711, J. Manion, P.I.), and Zach Holderfield assisted with the NMR measurements described above. The SSRL is supported by the Department of Energy, Office of Basic Energy Sciences.

Supporting Information Available: Crystallographic details including fractional atomic coordinates, thermal parameters, and complete listings of bond lengths and angles for Tp*NiBH$_4$ and Tp*NiCl in CIF format. This information is available free of charge via the Internet at http://pubs.acs.org.

IC034687A

(36) D. Rabinovich, private communication, June 2003.
(37) Carpenter, C. J.; van Koppen, P. A. M.; Bowers, M. T. *J. Am. Chem. Soc.* **2000**, *122*, 392.
(38) Haynes, C. L.; Chen, Y-. M.; Armentrout, P. B. *J. Phys. Chem.* **1996**, *100*, 111.